Available online at www.sciencedirect.com

ScienceDirect

journal homepage: http://www.elsevier.com/locate/acme

Original Research Article

Parameter identification of Bouc-Wen model for vacuum packed particles based on genetic algorithm

Piotr Bartkowski *, *Robert Zalewski*, *Paweł Chodkiewicz*

Warsaw University of Technology, Faculty of Automotive and Construction Machinery Engineering, Poland

ARTICLE INFO

Article history:
Received 30 July 2018
Received in revised form
19 October 2018
Accepted 11 November 2018
Available online 8 December 2018

Keywords:
Vacuum packed particles
Granular damper
Semi-active damping
Modeling
Experiments

ABSTRACT

This paper investigates cylindrical samples made of vacuum packed particles. Such structures are composed of granular media placed in a hermetic encapsulation where, in the final stage, a partial vacuum is generated. The main advantage of such a structure is that the underpressure value makes it possible to control the global physical properties of granular systems. Materials with various grains are analyzed in the paper. A modified Bouc-Wen hysteresis model is adopted to describe the nonlinear properties of the tested specimens. To identify the model parameters, a genetic algorithm is applied. The proposed model is found to be in good agreement with the experimental data.

1. Introduction

Damping of vibrations in various mechanical systems is still an object of interest for many engineers and researchers. Over the past few years, many solutions for vibration dampers that have the ability to control damping properties have appeared. Since the smart materials commercially available have significant drawbacks, which are described in the further part of the paper, the authors investigated a novel means of attentuating vibration using vacuum packed particles (VPP) as materials responsible for energy dissipation. VPPs are structures composed of loose grains packed in a sealed plastomeric container in which a partial vacuum is generated [1]. By changing the value of the pressure in the container, it is possible to adjust the macroscopic mechanical properties of the structure. The main disadvantages of popular 'intelligent materials' are their purchase price [2], complexity of auxiliary equipment, low durability [3] and limited working temperature range [4]. Many others scientists from around the world continue to search for innovative smart materials which would not have those drawbacks. Vacuum packed particles are inexpensive and it is relatively easy to control their mechanical properties, making them an attractive alternative to some of the smart structures that are currently used.

* *Corresponding author.*
E-mail addresses: bartkowski_piotr@onet.pl (P. Bartkowski), robertzalewski@wp.pl (R. Zalewski), pawel@chodkiewicz.com.pl (P. Chodkiewicz).

https://doi.org/10.1016/j.acme.2018.11.002
1644-9665/

The overall objective of the authors was to design a new controllable VPP damper that can replace popular magnetorheological devices in the field of vibration attenuation. To propose an effective and reliable control strategy for the damper prototype, an appropriate mathematical model is required. Since VPPs exhibit strongly nonlinear mechanical characteristics, the authors chose and modified the Bouc-Wen model to capture the behavior of VPPs as a core element of a future vibration damper prototype. In the following sections of this paper, that model, and the parameter identification procedure using a genetic algorithm, are presented. During the process of designing a vibration damper, various limitations – including maximum force values, design space and dissipation capability – are often imposed. Frequently, the materials are the only variable remaining. The authors decided to focus on investigating VPPs made of various granular materials to check the global effect of the grain material on the behavior of the entire structure.

As mentioned above, a controllable VPP damper seems to be an innovative and promising concept, while the engineering applications of VPPs can be widely found in the literature.

The first important engineering application of VPPs were 'vacuum mattresses' – therapeutic devices used to stabilize and transport injured patients [5]. Another use of granular conglomerates is in a flexible robot gripper that is able to pick up and carry various types of objects [6]. The gripper employs an expandable hermetic bag filled with a granular material (coffee grains). The system is 'jammed' by the application of a vacuum after contact so that the object can then be moved from one place to another. An interesting medical application of VPPs can be found in [7], where an innovative support for flexible endoscopes is investigated. The problem from the medical point of view is to provide a sufficiently rigid support for a flexible endoscope that must be inserted into the human body. For this purpose, a 'Vacu-SL' shaft guide is used. The guide is made of VPPs, and its biggest advantage is that its rigidity can be reduced when it is introduced into the body, significantly increasing patient comfort. When an underpressure is generated inside the system, the bending stiffness of the guide increases significantly. The paper referred to discusses various particle sizes and their impact on the global mechanical properties of endoscopes.

Another interesting application of VPPs is discussed in [8], where a shape-shifting ChemBot is introduced. Such a soft, morphile robot can move around as its external shape can be changed using what is known as 'jamming skin-enabled locomotion'. The skin of the device consists of hermetic cells filled with a granular material. Changing the underpressure inside those cells makes it possible to control their displacement, causing the ChemBot to move in the desired direction. Very interesting use of VPP as a soft robots with variable stiffness is described in paper [9].

Nowadays, vacuum packed particles are also used in semi-active systems for attenuating vibrations in slender elements. In papers [10,11] and [12] the authors showed that placing the metal beam inside a hermetic granular sleeve makes it possible to control the damping characteristics of such objects by an easily adjustable underpressure parameter.

An interesting construction of a VPP controllable linear damper is shown in [13] or [14]. The authors found similarities of the granular prototype to well commercialized MR devices. Changing the internal underpressure inside the granular core resulted in observable changes in the overall dissipative properties of granular shock absorbers. A similar solution is presented in [15], where a prototype of a multiaxial VPP shock absorber is presented. The biggest advantage of the proposed solution is the ability to control, by the underpressure value, the quasi-plastic flow of granular media. The impact energy is dissipated mostly by 'intergranular' friction forces, and the process is fully reversible by increasing the pressure inside the system.

Previous works of the authors showed that vacuum packed particles can be successfully incorporated as part of 'intelligent' sound absorbers. Changing the partial vacuum inside a plate made of a granular conglomerate affects its sound absorption coefficient. While the acoustic properties of VPPs are a function of underpressure, such structures seem promising as innovative materials in noise attenuation systems.

Concluding this review of VPP applications, it is worth mentioning that works describing their application in engineering are far ahead of publications on the process of modeling their mechanical properties. The presented paper addresses this issue.

In the next part of the paper the authors show the experimental results of their VPP specimen. The effects of grain material and underpressure value were studied. Section 3 covers modelling. The Bouc-Wen model is introduced, and its limitations in non-symmetrical hysteresis loops are discussed. Next, a proposed model modification is given. The parameter identification process using a genetic algorithm is reported in Section 3.2. A detailed discussion of the results is provided in Section 3.3. The conclusions and future directions for research are set out in Section 4.

2. Experimental

2.1. *Types of material*

In this paper, three types of granular materials were investigated experimentally: *PC/ABS C12HF*, *POM C 9021* and *POM MT24u01*. All the laboratory tests were carried out on ball-shaped grains having a diameter of about 3 mm (Fig. 1). Additionally, in Table 1, the basic mechanical properties of the materials, including Young modulus, yield stress and nominal strain at break, are presented.

Vacuum packed particles (VPPs) were tested in samples specially developed for this purpose. The grains were placed in a plastomer container made of polyethylene. A constant void fraction (porosity) of 34% was maintained during all the laboratory tests. The length and diameter of the samples were 100 mm and 50 mm, respectively. A typical experimental specimen is depicted in Fig. 2.

2.2. *Methods*

The granular samples were tested on a SHIMADZU EZ-LX testing machine equipped with a force load cell max of 5000 kN (Fig. 3). The samples were fixed in dedicated holders as

Fig. 1 – Tested grains.

Table 1 – Mechanical properties of the grain materials.

	Young modulus [MPa]	Yield stress [MPa]	Nominal strain at break [%]
PC/ABS C12HF	2360	55	>50
POM C 9021	2500	48	16
POM MT24u01	2900	65	17

Fig. 2 – Material sample.

Fig. 3 – Testing machine.

illustrated in Fig. 4. During the experiments, the time, yaw displacement and force were recorded. The tests were carried out assuming a constant quasi-static strain rate. The triangular excitation rule, assuming four full loading and unloading cycles, was considered (Fig. 5). Experiments were performed for five different underpressure values: 0.01 MPa, 0.03 MPa, 0.05 MPa, 0.07 MPa, 0.09 MPa. Additionally to check the repeatability of results each underpressure value and each material were tested three times. During the experiments 45 material samples were tested. The results of the experiments and the variation between the results are discussed in the next section.

2.3. *Results discussion*

In this part of the paper, the results of the experimental tests are presented. Engineering stress/strain curves for each material are presented in Figs. 6–9. To prove that the behavior of the VPP structures is repeatable, three individual experi-

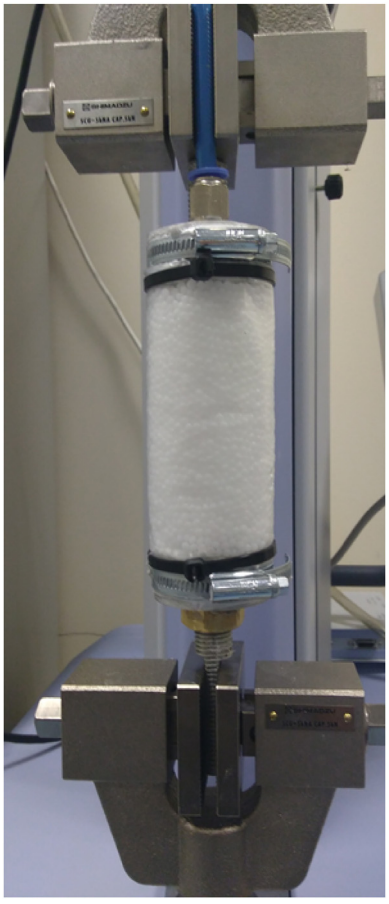

Fig. 4 – Sample mounted in the machine.

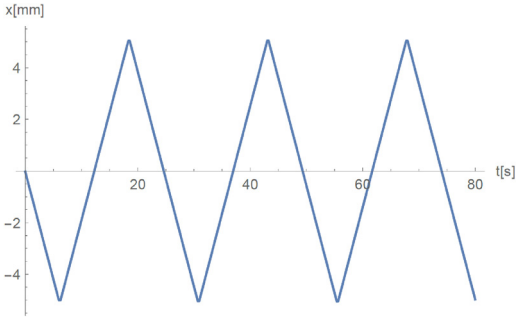

Fig. 5 – The triangular excitation.

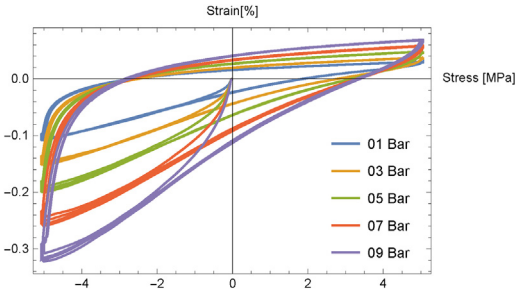

Fig. 6 – Stress/strain curve for POM C 9021.

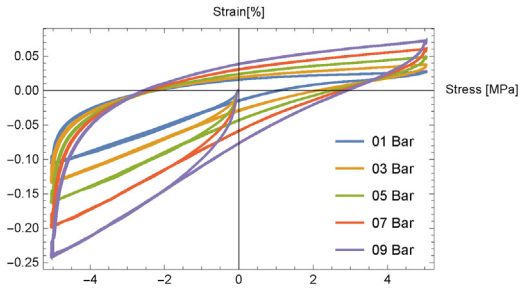

Fig. 7 – Stress/strain curve for POM MT24u01.

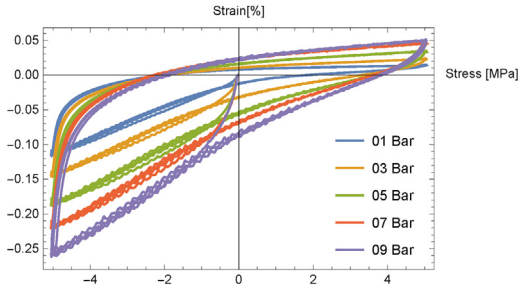

Fig. 8 – Stress/strain curve for PC ABS C12HF.

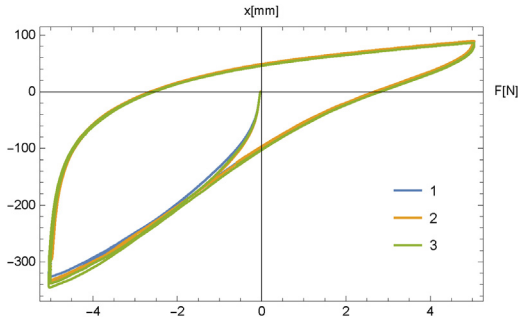

Fig. 9 – Force/displacement curve for three samples.

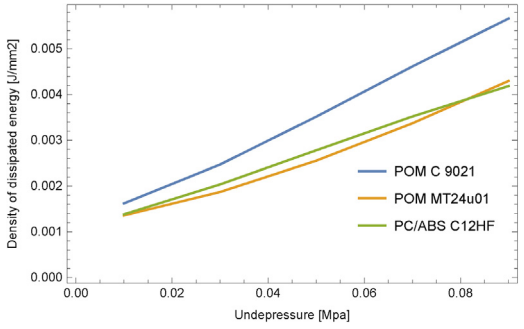

Fig. 10 – Density of dissipated energy.

mental series for the assumed configuration of the specimen (type of grain and underpressure) were conducted. Fig. 9 presents the results, force in function of displacement, recorded by the test stand, for one of the underpressure value performed for three material samples. It can be observed that the shapes of recorded hysteresis loops are similar. The values of determined material parameters including yield stress (0.2%), stress 5%, density of dissipated energy, revealed slight

Table 2 – Mechanical properties of the PC/ABS C12HF.

Undepressure value [MPa]	Yield stress (0.2%) [MPa]	Stress for 5% [MPa]	Absorbed energy
0.01	0.011	0.0.108	0.0014
0.03	0.017	0.0.132	0.002
0.05	0.022	0.0.187	0.0028
0.07	0.032	0.0.227	0.0035
0.09	0.04	0.0.262	0.0042

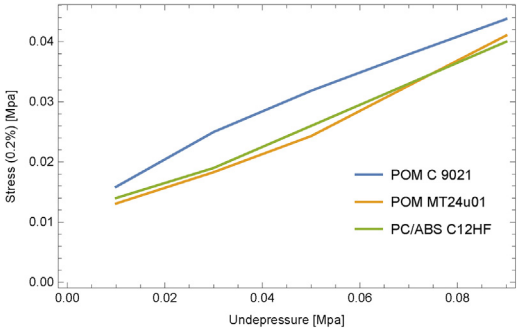

Fig. 11 – Stress for 0.2%.

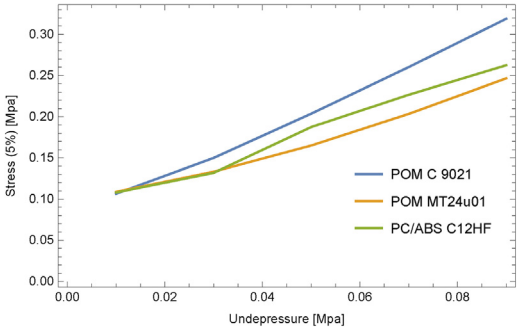

Fig. 12 – Stress for 5%.

differences not exceeding 7%. It confirms that the experimental data is repeatable, especially when such a complex material is consider. Typical experimental results are depicted in Fig. 10. Additionally, in Table 2, the basic mechanical properties of the material, including: yield stress (0.2%), stress 5%, density of dissipated energy (in 4 cycles) are presented (Figs. 11 and 12). As mentioned above, three different types of grain materials were tested. Despite their geometrical similarities, there were differences recorded in the shape of the cyclic loading loops, caused by variations in the grain mechanical properties. VPP structures made of POM C 9021 grains are characterized by strain curves of a similar shape for each material, therefore the density of the dissipated energy changes similarly to stress (5%). It is worth mentioning that a correlation was found between the yield stress of the grain material (Table 1) and the global mechanical properties of the whole VPP structure. The POM C9021 material exhibits the largest value of yield stress, and consequently, the VPPs made of this material displayed the highest value of 0.2% and 5% stress or dissipated energy. As mentioned in the introduction, VPPs can be used as materials for vibration damping. Analyzing the results of our experiments, it can be concluded that the POM C9021 samples have the best damping properties. The experimental results confirmed that it is possible to change the VPP damper parameters by changing the grain type, which can have very interesting practical applications (Tables 3 and 4).

3. Modeling

3.1. *Bouc-Wen model*

As can be seen in Figs. 6–8, the response of vacuum packed particles to the applied kinematic excitation rule is nonlinear and assymmetrical. Previous works of the authors revealed that VPPs are in some sense comparable to magnetorheological (MR) fluids and devices working on the basis thereof [1]. Therefore, the process of modelling granular structures was based on a suitable mathematical formula drawn from the wide range of models developed for MR fluids. Typically, the Bingham model is adopted to capture the basic features of MR devices. This model includes dry friction described as a signum function on the system velocity connected in parallel to a viscosity element [16–18]. Although the model has computational simplicity, it can reproduce only a limited number of the observed hysteresis characteristic shapes. A more complex approach to modelling the behavior of MR devices is the Gamota–Filisko model [19]. Besides being a Bingham body model, this model is a typical example of a Bingham model extension – a combination of Bingham, Kelvin-Voight and Hooke elements. It permits a description to be made of the behavior of a material in the pre-yield and post-yield regions.

Table 3 – Mechanical properties of the POM C 9021.

Undepressure value [MPa]	Yield stress (0.2%) [MPa]	Stress for 5% [MPa]	Absorbed energy
0.01	0.016	0.0.11	0.0016
0.03	0.025	0.0.15	0.0025
0.05	0.032	0.0.2	0.0035
0.07	0.038	0.0.26	0.0046
0.09	0.044	0.0.32	0.0057

Table 4 – Mechanical properties of the POM MT24u01.

Undepressure value [MPa]	Yield stress (0.2%) [MPa]	Stress for 5% [MPa]	Absorbed energy
0.01	0.013	0.0.109	0.0014
0.03	0.018	0.0.133	0.0019
0.05	0.024	0.0.165	0.0026
0.07	0.033	0.0.203	0.0034
0.09	0.041	0.0.247	0.0043

Also, the yield point can be captured. In the literature also other models that describe the hysteresis loop of physical phenomenon, including Jiles–Atherton hysteresis model [20,21] or Preisach model of hysteresis [22], can be found. It seems that the most popular model for capturing not only the mechanical hysteresis loops but also various physical systems, such as piezoelectrics, electrorheological fluids or magnetism, is the Bouc-Wen (B-W) model. It was initially proposed by Bouc [23] and later extended by Wen [24]. Because of the versatility of the B-W model in engineering applications, the authors decided to adopt it to capture the behavior of VPPs. The model takes into account a differential equation to represent the non-linear response of the described system. Additionally, it displays reasonable complexity, and can be widely applied in various control strategies. The disadvantage of the model is its nonlinear nature, the relatively large number of parameters, and a very high sensitivity of response to small changes in parameter values. Nowadays, thanks to the development of numerical algorithms, calibrating the B-W model no longer seems to be a problem.

In this paper, the Bouc-Wen formulation is used for the classical inverse problem, where the input data is the set of experimentally recorded characteristics and the required output is a set of model parameters that will successfully reproduce the actual features of special granular structures.

The original Bouc-Wen model consists of seven material parameters that have to be identified based on the experimental results. The biggest problem is that the classical formulation of the B-W model does not reflect the nonsymmetrical hysteresis loops observed for the VPPs under discussion. Consequently, the authors proposed a modification of the B-W model to make it possible to capture the real behavior of the VPPs. The original Bouc-Wen model is a system of non-linear differential equations described as:

$$\begin{cases} \ddot{x} + 2\xi\omega_n\dot{x} + \alpha\omega_n^2 x + (1-\alpha)\omega_n z = u(t) \\ \dot{z} = -\gamma|\dot{x}||z|^{n-1}z - \beta\dot{x}|z|^n + A\dot{x} \end{cases} \quad (1)$$

where $u(t)$ is a forcing function. Based on [2] the model parameters can be described as: rigidity ratio, $\alpha(0\leq\alpha\leq1)$, linear elastic viscous damping ratio, $\xi(0\leq\xi\leq1)$, pseudo-natural frequency of the system, ω_n (in rad/s), hysteresis amplitude controlling parameter, A, and hysteresis loop shape controlling parameters β, γ and $n(n\geq1)$.

The variable z is responsible for the shape of the simulated hysteresis loop. It represents the artificial displacement connected to the actual displacement (x). A schematic representation of the B-W model and a typical shape of the hysteresis loop that can be captured by it are depicted in Fig. 13

To capture the real assymmetrical hysteresis loops recorded for the VPPs, the authors proposed a certain modification of the original B-W model. It was previously shown that the mechanical response of the granular systems considered strongly depends on the direction of the velocity. Therefore, the authors assumed that different values of the model parameters for the elongation and compression processes. Such an approach modified the model formulas as follows:

$$\ddot{x} + 2\xi_+\omega_{n_+}\dot{x} + \alpha_+\omega_{n_+}^2 x + (1-\alpha_+)\omega_{n_+}^2 z_+ = F \quad \text{for} \quad \dot{x}\geq0 \quad (2)$$

$$\ddot{x} + 2\xi_-\omega_{n_-}\dot{x} + \alpha_-\omega_{n_-}^2 x + (1-\alpha_-)\omega_{n_-}^2 z_- = F \text{ for } \dot{x}<0 \quad (3)$$

where displacements z_+ and z_- are described as:

$$\dot{z}_+ = -\gamma_+\cdot z_+\cdot|\dot{x}|\cdot|z_+|^{n-1} - \beta_+\cdot\dot{x}\cdot|z_+|^n + A_+\cdot\dot{x} \text{ for } \dot{x}\geq0 \quad (4)$$

$$\dot{z}_- = -\gamma_-\cdot z_-\cdot|\dot{x}|\cdot|z_-|^{n-1} - \beta_-\cdot\dot{x}\cdot|z_-|^n + A_-\cdot\dot{x} \text{ for } \dot{x}<0 \quad (5)$$

The lower index '+' in the above formula corresponds to the ''tensile test'', consequently, index '-' is related to the compression process of the VPPs. The modified B-W model given by Eqs. (2) and (3) makes it possible to determine the assymmetrical hysteresis loops, assuming different values of the model parameters. Analyzing the modified B-W model for VPP structures, one can state that it consists of 14 material parameters that must be identified based on the experimental results. The classical inverse problem consisting of identifying the model parameters is most often solved numerically using heuristic methods where the typical examples include Particles Swarm Optimization [25], Firefly Algorithm [26], Simulated Annealing [27] or Evolutionary Algorithm [28].

3.2. *Genetic algorithm*

The authors used genetic algorithms (GAs) to identify 14 parameters of the modified Bouc-Wen model. GAs are a non-deterministic optimization method based on real organisms present in nature, modelled by Darwinian biological evolution model. The evolution is simulated using a set of biologically inspired operators (like selection, crossover, mutation). In this process, better individuals have more chances to survive and to form next generations.

The history of the GA began in 1957, when quantitative geneticist Alex Fraser started publishing a series of papers on simulating the artificial selection of organisms [29]. In the early

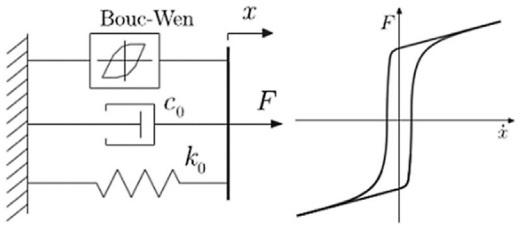

Fig. 13 – The schematic representation of the B-W model and the typical hysteresis loop.

1960s, these methods were described in Fraser et al. [30]. Fraser's simulations used all of the elements of genetic algorithms. In the first developments of GAs binary strings were used to code individuals [31]. Recent practices mostly code the solutions using real numbers [32], and operational efficiencies are improved. There are also several problem-dependent control parameters, e.g., crossover and mutation rate that required to be specified. It is also difficult to define the termination criteria for the algorithm.

Nowadays, those methods are implemented in particular in the machine learning process [33,34], combinatorial optimization [35], mechanical modelling [36,37], the modelling of smart materials [1,38] and many other areas.

In this paper, a population of 100 individuals represented as the real numbers, was used to predict the values of the model parameters. The parameters were divided into two groups according to strain rate direction. Seven parameters correspond to a positive strain rate value and are related to an elongation of the VPP specimen (A_+, n_+, α_+, β_+, γ_+, ξ_+, ω_{n_+}). The other group of parameters reflects the compressed behavior of the investigated samples (negative strain rate value) (A_-, n_-, α_-, β_-, γ_-, ξ_-, ω_{n_-}). The GA procedure was programmed in the Wolfram Mathematica environment.

A block diagram of the procedure is presented in Fig. 14.

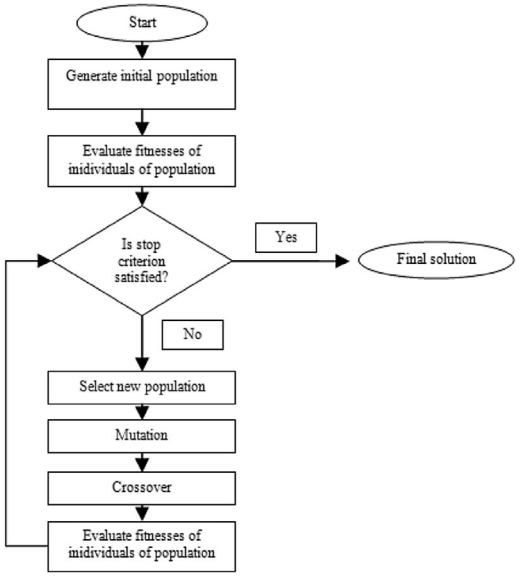

Fig. 14 – Block diagram of algorithm used to find parameters of Bouc-Wen model.

No	F_{err}	A_+	n_+	α_+	β_+	γ_+	ξ_+	ω_{n_+}
		A_-	n_-	α_-	β_-	γ_-	ξ_-	ω_{n_-}

Fig. 15 – Sample of individuals used in algorithm.

The first step of the algorithm is to create a population of individuals. We used the individuals to calibrate the modified Bouc-Wen model, constructed as 16 numeric fields. The meaning of the fields is presented in Fig. 15.

The fitness function F_{err} was used to describe the level of success of the model solution with parameters from the individuals.

$$F_{err} = -1\frac{(F_m - F_{eks})(F_m - F_{eks})}{L} \tag{6}$$

$$\mathrm{F_m} = (F^1, F^2, \ldots, F^t), \qquad \mathrm{F_{eks}} = (F_e^1, F_e^2, \ldots, F_e^t) \tag{7}$$

where: t - time of simulation/experiment; F^t – value of force simulation in t-time; F_e^t – value of force from experiment in t-time; L – length of vector.

In the population, 100 individuals were taken into account. The first values of the individual fields were chosen randomly, within the range shown in Table 5.

In the next step of the algorithm, the fitness function is calculated for all individuals. The iterative simulation of evolution steps starts with a selection of individuals with a ''better'' (lower value) F_{err} value for the next procedure. The authors chose a tournament selection. In this procedure two individuals from the population are selected randomly and the one that had a better fitness function value is taken to the new population. Then, in the evolution loop, all new individuals were mutated. This operation randomly chooses one parameter (e.g. β_-) from an individual and modifies by replacing the selected value by a new one randomly generated within the range of parameter variation. This operation depends on the result of mutation indicator related to probability of mutation, that was set to 50%. The next step is called 'crossover' applied to a pair chosen individuals. This operation involves switching of one selected parameter between the strings of individuals. Similarly, the crossover probability was set to 50%. After those two steps the fitness function is calculated and a new population composed of best solutions is created. During this algorithm the number of individuals is constant. As the stop criteria, the authors chosen a total number of algorithm loops (40 loops was proposed, after several tests). The typical convergence plot of the fitness function vs number of iterations for PC/ABS material subjected to 0.09 MPa is depicted in Fig. 16. Including a larger number of generations in the algorithm did not lead to significant changes in the determined values of the objective function.

3.3. *Results discussion*

The 14-parameter modified Bouc-Wen model represents relatively well the real behavior of VPP samples subjected to

Table 5 – Range of start values of parameters for individuals.

Parameter	Start value	End value	Parameter	Start value	End value
A_+	0.001	0.025	A_-	0.05	1.25
n_+	0.43	10.75	n_-	0.2	5.
α_+	0.07	1.75	α_-	0.0055	0.1375
β_+	0.1	2.5	β_-	0.001	0.025
γ_+	0.3	7.5	γ_-	0.2	5.
ξ_+	20.	500.	ξ_-	−23.	−575.
ω_{n_+}	0.3	7.5	ω_{n_-}	1.8	45.

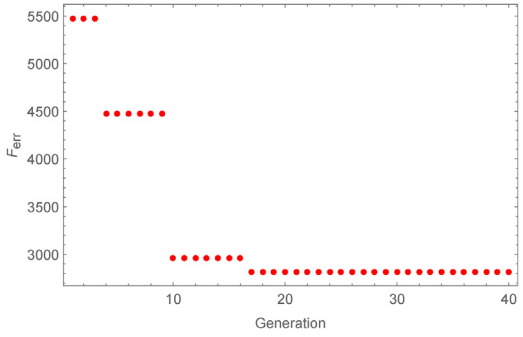

Fig. 16 – Optimal fitness function value vs generation number.

the triangular excitation rule. It has to be noted that the experimentally induced displacement slightly differed from the sine type approximation function taken into consideration in the numerical analysis. This approach was chosen to simplify the calculations of the first and second derivatives of the excitation rules. However, the type of displacement applied in the laboratory tests makes it possible to omit the inertia forces (in the case under discussion, we observed a partially constant speed and did not notice any acceleration in the system), limiting the dynamical response of the B-W model. The differences are particularly important in the regions, where a change in the velocity directions exists (Fig. 17).

Obviously, the error between the model response and the experimental data is mostly observable in the regions of extreme excitation values.

After finalizing the identification processes of the B-W model for various values of underpressure, the authors looked for unambiguous trends in the changes in the values of the model parameters as a function of underpressure. The GA search method proposes a set of parameters that can vary somewhat due to the stochastic nature of the strategy implemented, but which mostly correctly fit the experimental results. Based on the data depicted in Fig. 18 it can be stated that, at this stage of the research, this seems to be very problematic. It is true that in the parameters illustrated in Fig. 19 one can observe a dependency between the acquired parameters value and the partial vacuum, but globally introducing the underpressure parameter to the B-W model would seem to be premature at this point (Tables 6–8 and Figs. 20 and 21).

4. Conclusion

The features of VPPs have been investigated for several years, and the engineering applications of these extraordinary granular conglomerates are ahead of the modelling process. The behavior of the systems discussed is complex, and the experimentally recorded hysteresis loops are assymmetrical. The physico-mechanical processes occurring in VPPs in operation are not fully recognized. In this paper, the cyclic loading of typical, cylindrical VPP samples filled with various grains was studied. A modified Bouc-Wen model was applied to capture the inelastic deformation of the structures investigated. The relationship between the B-W model response and the experimental data showed the ability of the model to take into consideration the highly nonlinear

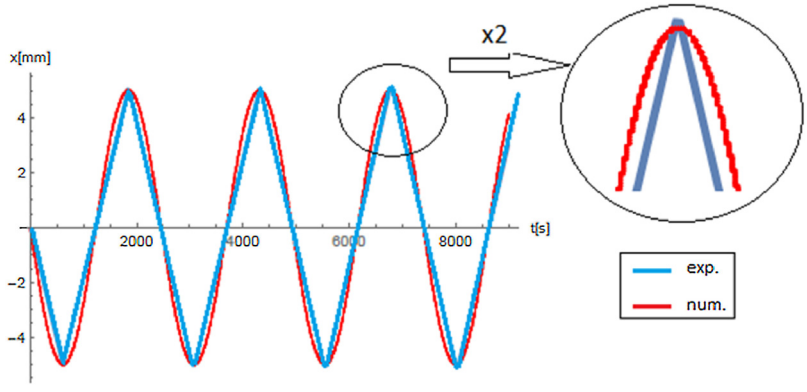

Fig. 17 – Differences in an experimental and numerical excitation rules.

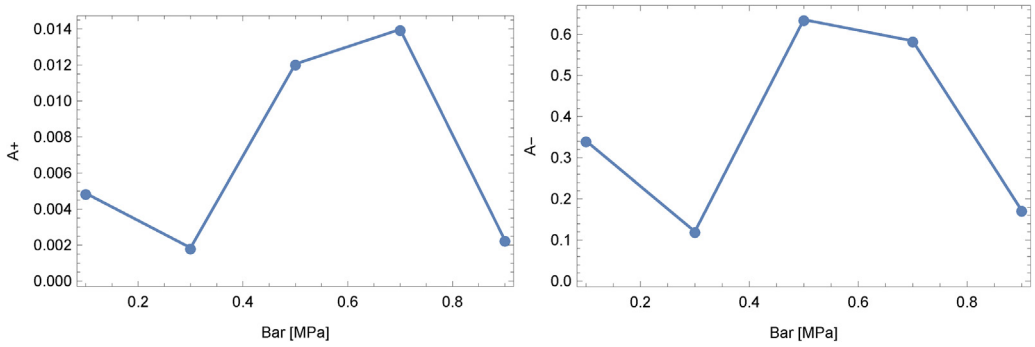

Fig. 18 – Parameters for Bouc-Wen model – POM MT24u01.

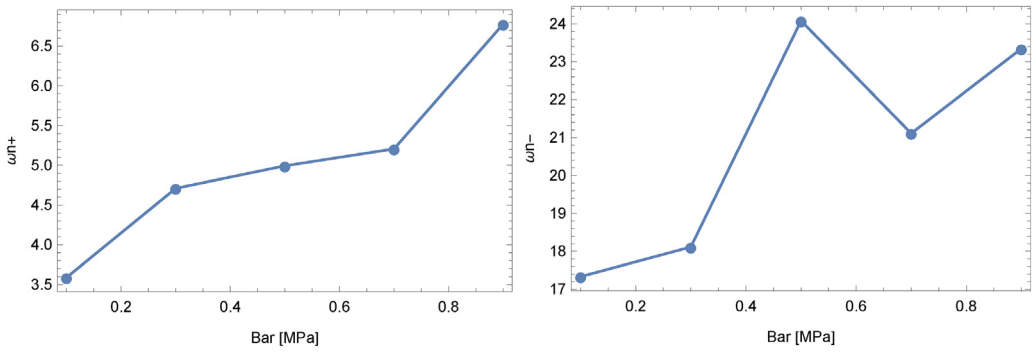

Fig. 19 – Parameters for Bouc-Wen model – POM MT24u01.

Table 6 – Parameters for POM MT24u01 material.

Undepressure value [MPa]	F_{err}	A''_+	n_+	α_+	β_+	γ_+	ξ_+	ω_{n_+}
0.01	−833.793	0.005	5.019	1.009	1.171	3.600	261.893	3.589
0.03	−609.061	0.002	6.667	0.979	0.359	3.110	400.935	4.711
0.05	−2796.644	0.012	7.313	1.120	1.631	1.417	230.757	4.994
0.07	−2294.602	0.014	3.067	1.481	1.263	2.285	276.255	5.207
0.09	−2780.160	0.002	5.649	0.879	0.854	7.006	331.905	6.778
Undepressure value [MPa]	F_{err}	A_-	n_-	α_-	β_-	γ_-	ξ_-	ω_{n_-}
0.01	−833.793	0.341	2.825	0.068	0.014	2.814	−151.740	17.333
0.03	−609.061	0.121	2.477	0.101	0.004	2.047	−32.796	18.113
0.05	−2796.644	0.636	2.120	0.066	0.014	2.924	−166.532	24.082
0.07	−2294.602	0.584	4.932	0.075	0.006	2.600	−318.414	21.111
0.09	−2780.160	0.173	3.548	0.089	0.014	2.249	−129.033	23.345

Table 7 – Parameters for POM C9021 material.

Undepressure value [MPa]	F_{err}	A''_+	n_+	α_+	β_+	γ_+	ξ_+	ω_{n_+}
0.01	−731.706	0.002	9.650	0.745	2.295	4.348	209.898	4.871
0.03	−1510.412	0.012	9.632	0.331	1.438	2.457	458.330	7.470
0.05	−2029.619	0.025	8.414	0.601	2.329	5.309	234.400	5.810
0.07	−2283.016	0.019	10.057	0.869	2.036	3.851	112.993	5.763
0.09	−3432.456	0.017	5.649	0.879	1.132	1.324	331.905	4.891
Undepressure value [MPa]	F_{err}	A_-	n_-	α_-	β_-	γ_-	ξ_-	ω_{n_-}
0.01	−731.706	0.492	4.438	0.107	0.019	4.646	−276.411	15.408
0.03	−1510.412	0.532	4.430	0.110	0.005	4.586	−291.547	18.172
0.05	−2029.619	0.962	1.883	0.061	0.005	1.417	−433.678	20.767
0.07	−2283.016	0.648	1.954	0.080	0.005	4.691	−94.900	26.217
0.09	−3432.456	0.435	3.548	0.089	0.010	2.358	−289.630	23.345

Table 8 – Parameters for PC/ABS C12HF material.

Undepressure value [MPa]	F_{err}	A''_{+}	n_{+}	α_{+}	β_{+}	γ_{+}	ξ_{+}	$\omega_{n_{+}}$
0.01	−540.960	0.011	4.351	0.577	2.452	5.231	152.329	5.049
0.03	−1266.001	0.003	6.906	0.714	1.279	5.492	304.154	6.454
0.05	−2098.454	0.020	9.879	0.989	0.566	0.625	209.898	5.600
0.07	−3885.284	0.007	4.835	0.594	1.300	7.404	389.219	7.146
0.09	−5495.133	0.006	9.128	1.619	0.579	4.190	443.416	5.367

Undepressure value [MPa]	F_{err}	A_{-}	n_{-}	α_{-}	β_{-}	γ_{-}	ξ_{-}	$\omega_{n_{-}}$
0.01	−540.960	0.717	0.466	0.028	0.024	1.952	−54.433	31.888
0.03	−1266.001	1.164	1.827	0.121	0.002	1.071	−280.869	15.525
0.05	−2098.454	0.195	2.891	0.061	0.017	3.553	−68.228	25.979
0.07	−3885.284	0.322	4.722	0.106	0.004	2.259	−111.663	21.407
0.09	−5495.133	0.546	3.496	0.130	0.011	2.870	−111.330	23.795

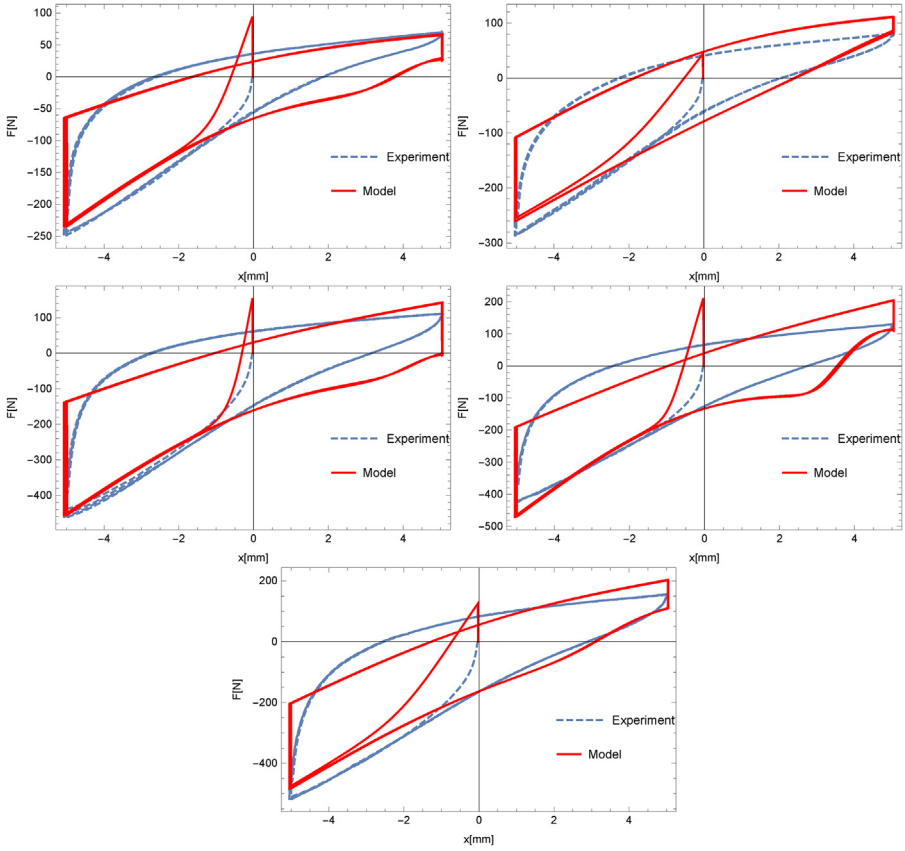

Fig. 20 – POM MT24u01 – experiment vs model.

features and velocity-direction dependence of those structures. The model parameters were determined numerically. The calibration process was formulated as an optimization problem, and solved using a GA implemented in the Mathematica environment. The GA is a random search method, and its effectiveness in the inverse problem of identifying model parameters for the VPPs was found to be effective. The main disadvantage of this methodology consists in the large number of potential optimal solutions that have to be considered to obtain a final outcome. For the numerical results discussed in this paper, the CPU time on a personal computer was quite reasonable, and varied between 30 and 45 min for a single algorithm run (PC with Processor Intel Core i7-6700HQ and 16 GB memory was used for the stimulations made in Mathematica 11 environment). The presented approach can be easily applied to other multi-parameter models or constitutive laws developed or modified to capture the properties of novel materials or structures. Based on the experimental data and numerical simulation results, it can be stated that, for an accurate calibration of the Bouc-Wen model, more GA runs should be performed. At the current stage of VPP investigations it is impossible to propose universal relationships between the B-W model parameters and the value of the partial vacuum generated inside the system. Also, cyclic

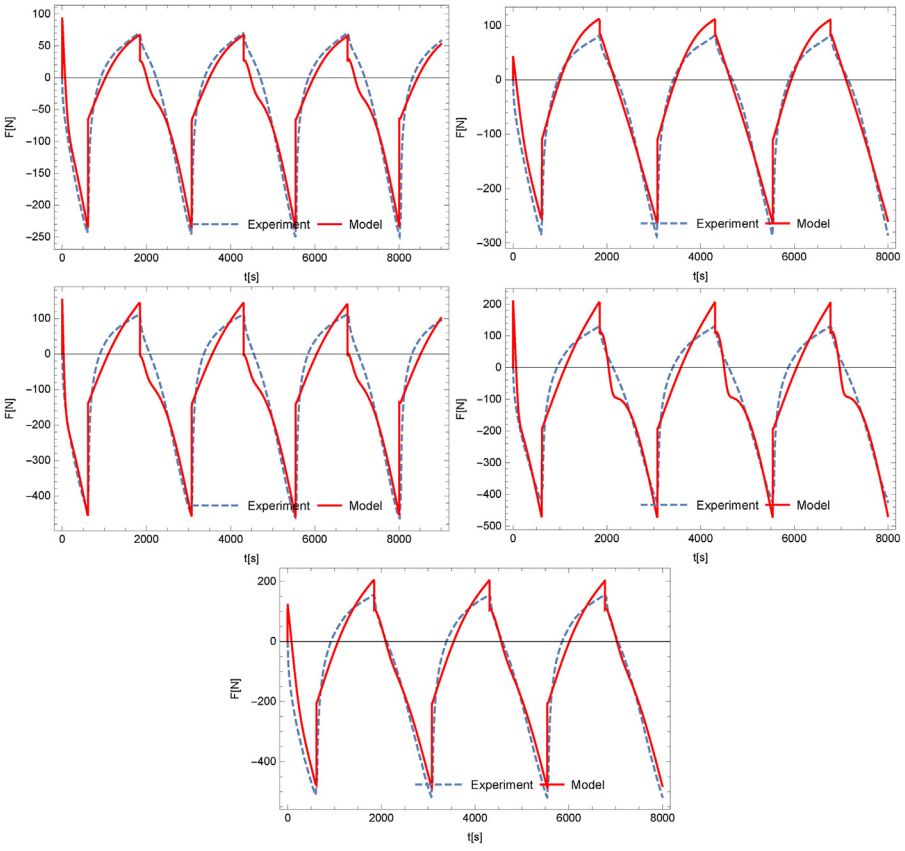

Fig. 21 – POM MT24u01 – experiment vs model.

loading loops obtained for various strain rates should be carried out. In future studies, a methodology similar to that presented in this paper will be applied in order to analyze different rheological models. Also, additional features of vacuum packed particles, such as time-dependent response, temperature or environmental impact, will be investigated. Improving the Bouc-Wen model by introducing an under-pressure parameter into the current mathematical formula may require supplementary experimental research in order to enhance the uniqueness of the solution and to ensure the correctness of the identification process.

Acknowledgements

This work was carried out within the project no. 2016/23/N/ST8/02056 founded by National Science Centre, Poland.

REFERENCES

[1] R. Zalewski, P. Chodkiewicz, Gubanov model for vacuum packed particles, in: Mechatronics 2013, Springer, 2014 57–63.
[2] P. Chodkiewicz, J. Lengiewicz, R. Zalewski, DEM modeling of Vacuum Packed Particles Damper, 2018.
[3] Y. Parepalli, S. Reddy Pamanji, M. CHAVALI, An overview of smart materials in nanoscience and nanotechnology, Int. J. Nanosci. Nanotechnol. 3 (2014) 9–14.
[4] J. Wang, G. Meng, Magnetorheological fluid devices: principles, characteristics and applications in mechanical engineering., Proc. Inst. Mech. Eng. L: J. Mater. Des. Appl. (2001) 165–174.
[5] M. Luscombe, J. Williams, Comparison of a long spinal board and vacuum mattress for spinal immobilisation, Emerg. Med. J. 20 (5) (2003) 476–478.
[6] E. Brown, N. Rodenberg, J. Amend, A. Mozeika, E. Steltz, M.R. Zakin, H. Lipson, H.M. Jaeger, Universal robotic gripper based on the jamming of granular material, Proc. Natl. Acad. Sci. 107 (44) (2010) 18809–18814.
[7] A.J. Loeve, O.S. van de Ven, J.G. Vogel, P. Breedveld, J. Dankelman, Vacuum packed particles as flexible endoscope guides with controllable rigidity, Granular Matter 12 (6) (2010) 543–554.
[8] A. Mozeika, E. Steltz, M.H. Jaeger, The first steps of a robot based on jamming skin enabled locomotion, in: IEEE/RSJ International Conference on Intelligent Robots and Systems, 2009, 408–409.
[9] A. Jiang, T. Aste, P. Dasgupta, K. Althoefer, T. Nanayakkara, Granular Jamming with Hydraulic Control, 2013.
[10] R. Zalewski, T. Szmidt, Application of special granular structures for semi-active damping of lateral beam vibrations, Eng. Struct. 65 (2014) 13–20.
[11] J. Bajkowski, B. Dyniewicz, C. Bajer, Corrigendum to "damping properties of a beam with vacuum-packed granular damper" [J. Sound Vib. 341 (2015) 74–85], J. Sound Vib. (2016) 377.

[12] T. Szmidt, R. Zalewski, Inertially excited beam vibrations damped by vacuum packed particles, Smart Mater. Struct. 23 (10) (2014) 105026.
[13] R. Zalewski, P. Chodkiewicz, Semi-active linear vacuum packed particles damper, J. Theor. Appl. Mech. 54 (1) (2016) 311–316.
[14] R. Zalewski, P. Chodkiewicz, M. Shillor, Vibrations of a mass-spring system using a granular-material damper, Appl. Math. Modell. 40 (17-18) (2016) 8033–8047.
[15] P. Bartkowski, R. Zalewski, A concept of smart multiaxial impact damper made of vacuum packed particles, in: MATEC Web of Conferences, page 05001. EDP Sciences, (2018) 157.
[16] B. Spencer Jr., S. Dyke, M. Sain, J. Carlson, Phenomenological model for magnetorheological dampers, J. Eng. Mech. 123 (3) (1997) 230–238.
[17] T. Butz, O. Von Stryk, Modelling and simulation of electro- and magnetorheological fluid dampers, ZAMM-Journal of Applied Mathematics and Mechanics/Zeitschrift für Angewandte Mathematik und Mechanik: Applied Mathematics and Mechanics 82 (1) (2002) 3–20.
[18] G. Yang, B.F. Spencer Jr., H.-J. Jung, J.D. Carlson, Dynamic modeling of large-scale magnetorheological damper systems for civil engineering applications, J. Eng. Mech. 130 (9) (2004) 1107–1114.
[19] D. Gamota, F. Filisko, Dynamic mechanical studies of electrorheological materials: moderate frequencies, J. Rheol. 35 (3) (1991) 399–425.
[20] D. Lederer, H. Igarashi, A. Kost, T. Honma, On the parameter identification and application of the Jiles-Atherton hysteresis model for numerical modeling of measured characteristics, IEEE Trans. Magnet. 35 (1999) 1211–1214.
[21] M. Asif Zaman, C. Hansen, P.T. Neustock, L. Padhy, P.L. Hesselink, Adjoint Method for Estimating Jiles-Atherton Hysteresis Model Parameters, 120, 2016, . p. 093903.
[22] G. Bertotti, Dynamic generalization of the scalar Preisach model of hysteresis, IEEE Trans. Magnet. 28 (1992) 2599–2601.
[23] R. Bouc, Forced vibrations of mechanical systems with hysteresis, in: Proceedings of the Fourth Conference on Nonlinear Oscillations, Prague, (1967) 1967.
[24] Y.-K. Wen, Method for random vibration of hysteretic systems, J. Eng. Mech. Div. 102 (2) (1976) 249–263.
[25] M. Ye, X. Wang, Parameter estimation of the Bouc-Wen hysteresis model using particle swarm optimization, Smart Mater. Struct. 16 (2007) 2341.
[26] M. Asif Zaman, U. Sikder, Bouc-Wen hysteresis model identification using modified firefly algorithm, J. Magnet. Magnet. Mater. 395 (2015) 229–233.
[27] S. Kirkpatrick, D. Gelatt Jr., P.M. Vecchi, Optimization by simulated annealing, Science 220 (1983) 671–680.
[28] M. Pyrz, M. Krzywoblocki, Crashworthiness optimization of thin-walled tubes using macro element method and evolutionary algorithm, Thin-Walled Struct. 112 (2017) 12–19.
[29] A.S. Fraser, Simulation of genetic systems by automatic digital computers i. introduction, Aust. J. Biol. Sci. 10 (4) (1957) 484–491.
[30] A. Fraser, D. Burnell, et al., Computer Models in Genetics, 1970.
[31] J. Holland, D. Goldberg, Genetic Algorithms in Search, Optimization and Machine Learning, Addison-Wesley, Massachusetts, 1989.
[32] Z. Michalewicz, Evolution strategies and other methods, in: Genetic Algorithms + Data Structures = Evolution Programs, Springer, 1996 159–177.
[33] J.J. Grefenstette, Genetic algorithms and machine learning., in: Proceedings of the Sixth Annual Conference on Computational Learning Theory, ACM, (1993) 3–4.
[34] J. Shapiro, Genetic algorithms in machine learning, in: Advanced Course on Artificial Intelligence, Springer, 1999 146–168.
[35] C. Reeves, Genetic algorithms and combinatorial optimization, Appl. Modern Heuristic Methods 111 (1995) 126.
[36] M. Pyrz, F. Zairi, Identification of viscoplastic parameters of phenomenological constitutive equations for polymers by deterministic and evolutionary approach, Model. Simul. Mater. Sci. Eng. 15 (2) (2007) 85.
[37] J. Zhou, B. Wang, J. Lin, L. Fu, Optimization of aluminum alloy anti-collision side beam hot stamping process using multi-objective genetic algorithm, Arch. Civil Mech. Eng. 13 (2013) 401–411.
[38] R. Zalewski, P. Chodkiewicz, M. Pyrz, Modeling of complex properties of vacuum packed particles using evolutionary algorithms, in: New Contributions in Information Systems and Technologies, Springer, 2015 267–276.